Modelling the epidemiology of residual *Plasmodium vivax* malaria in a heterogeneous host population: a case study in the Amazon Basin

Rodrigo M. Corder[1]*, Marcelo U. Ferreira[1#] and M. Gabriela M. Gomes[2,3]*#

[1]Department of Parasitology, Institute of Biomedical Sciences, University of São Paulo, São Paulo, Brazil

[2]Liverpool School of Tropical Medicine, Liverpool, United Kingdom.

[3]CIBIO-InBIO, Centro de Investigação em Biodiversidade e Recursos Genéticos, and CMUP, Centro de Matemática da Universidade do Porto, Porto, Portugal.

[#]These authors contributed equally.

*Correspondence: rodrigo.corder@usp.br or Gabriela.Gomes@lstmed.ac.uk

Abstract

The overall malaria burden in the Americas has decreased dramatically over the past two decades, but residual transmission pockets persist across the Amazon Basin, where *Plasmodium vivax* is the predominant infecting species. Current elimination efforts require a better quantitative understanding of malaria transmission dynamics for planning, monitoring, and evaluating interventions at the community level. This can be achieved with mathematical models that properly account for risk heterogeneity in communities approaching elimination, where few individuals disproportionately contribute to overall malaria prevalence, morbidity, and onwards transmission. Here we analyse demographic information combined with routinely collected malaria morbidity data from the town of Mâncio Lima, the main urban transmission hotspot of Brazil. We estimate the proportion of high-risk subjects in the host population by fitting compartmental susceptible-infected-susceptible (SIS) transmission models simultaneously to age-stratified vivax malaria incidence densities and the frequency distribution of *P. vivax* malaria attacks experienced by each individual over 12 months. Simulations with the best-fitting SIS model indicate that 20% of the hosts contribute 86% of the overall vivax malaria burden. Despite the low overall force of infection typically found in the Amazon, about one order of magnitude lower than that in rural Africa, high-risk individuals gradually develop clinical immunity following repeated infections and eventually constitute a substantial infectious reservoir comprised of asymptomatic parasite carriers that is overlooked by routine surveillance but likely fuels onwards malaria transmission. High-risk individuals therefore represent a priority target for more intensive and effective interventions that may not be readily delivered to the entire community.

Keywords: Mathematical modelling, urban malaria, heterogeneity, Amazon, hotspots, asymptomatic infection.

Author summary

Malaria transmission models that disregard risk heterogeneity at the community level, classifying individuals as uniformly susceptible or infected, may not properly recapitulate the epidemiology of malaria in real-life settings. Here we fit a compartmental susceptible-infected-susceptible model to malaria morbidity data from Mâncio Lima, the main urban transmission hotspot of Brazil, and estimate that 20% of the urban residents contribute 86% of the overall vivax malaria burden in the town. Despite the low average force of infection, one order of magnitude lower that in rural Africa, high-risk individuals experience enough repeated infections to develop clinical immunity and constitute an asymptomatic reservoir that fuels onwards malaria transmission. Therefore, these high-risk subjects account for the paradoxical finding of clinical immunity and frequent asymptomatic parasite carriage in low-endemicity Amazonian communities. We argue that mathematical models accounting for risk heterogeneity are crucial to plan and evaluate malaria control and elimination interventions targeted to high-risk groups in communities, municipalities, and regions.

Introduction

Heterogeneity in the risk of infection with several pathogens has been repeatedly documented in human populations, with 20% of the hosts typically harbouring 80% of the pathogen burden in the community [1]. For example, residents in the same village in rural Africa may greatly

59 differ in their malaria risk, leading to over-dispersed frequency distributions of malaria attacks
60 per person over time, with few subjects in the community experiencing frequent infection and
61 disease [2].
62
63 One source of malaria risk heterogeneity is the varying hosts' exposure to the pathogen, which
64 can be measured as the number of infectious mosquito bites per host per unit of time, termed
65 the entomological inoculation rate (EIR). About 20% of the children are estimated to receive
66 80% of all infectious mosquito bites in rural African settings, suggesting that malaria parasites
67 may also conform to the "20/80 rule" [3]. Significant malaria risk heterogeneity has also been
68 described in towns and cities in Africa [4-6]. For example, EIRs across the city of Brazzaville
69 were estimated in the early 1980s to range between <1 every three years and >100 per year
70 [7]. Not surprisingly, community-wide EIR measurements are affected by a range of
71 environmental factors (e.g., proximity of houses to water bodies that serve as larval habitats
72 for vectors), behavioural characteristics of individuals (e.g., occupational exposure to
73 mosquitoes and patterns of bednet use), and individual differences in attractiveness to
74 mosquitoes [e.g., 8]. Variation in overall malaria risk may also result from differences in
75 individual susceptibility to infection and subsequent disease given exposure, due to innate
76 resistance and acquired immunity developing after repeated infections [9].
77
78 A quantitative understanding of malaria transmission dynamics is required for planning,
79 monitoring, and evaluating interventions aimed at its elimination [10]. However, classical
80 susceptible-infected-susceptible (SIS) malaria models often disregard, totally or partially, risk
81 heterogeneity at the community level and classify hosts as more uniformly susceptible or
82 infectious than they actually are. Models that take insufficient account of real-world

heterogeneities may not properly recapitulate the transmission dynamics of malaria in endemic settings, in addition to not providing insights into the impact of targeting control interventions to high-risk groups [1, 10]. SIS models of infectious diseases may incorporate risk heterogeneity among hosts as, for example, a continuous distribution of hosts' susceptibility to infection, which can be determined empirically from the proportions of hosts that are experimentally infected at different pathogen challenge doses [11-13]. Alternatively, models may assume that the population of susceptible individuals is divided into a finite number of susceptibility classes or frailty groups [13-17].

The incidence of malaria in the Americas has decreased dramatically over the past two decades, but residual transmission pockets persist across the Amazon and challenge current elimination efforts. Residual malaria refers to the transmission that persists despite achieving high coverage of effective control measures such as use of insecticide-treated bednets and indoor residual spraying [18]. *Plasmodium vivax*, the predominant human malaria parasite in the region, is found in nearly 76% of cases in this continent [19]. Here, we fit compartmental SIS models that incorporate risk heterogeneity to malaria surveillance data, aiming to explore the transmission dynamics of *P. vivax* in the main urban malaria hotspot of the Amazon Basin of Brazil.

Results

A homogeneous-risk model does not satisfactorily recapitulate the epidemiology of *Plasmodium vivax* malaria

We first fitted empirical data by using a compartmental SIS model that considers the entire host population as being homogeneously at risk ($p_1 = 1$ and $x_1 = 1$; parameters are described in Materials and Methods section) of clinical vivax malaria (Fig 1C). The simultaneous fitting to empirical profiles of incidence by age and number of annual episodes per person (parameter estimation process is fully described in S1 File) is optimal when the age-dependent force of infection (Equation 1) takes parameter values $\lambda_0 = 0.7452$, $c = 0.8787$ and $k = 0.0282$ (Fig 1D) and the partial immunity factor (Equation 2) decays at constant rate $\alpha = 0.1162$ per infection experienced (Fig 1E). The homogeneous-risk model output recapitulates how malaria incidence density varies with age (Fig 1A; see also [20]) but does not satisfactorily fit the number of episodes per person over the one-year follow-up (Fig 1B).

Fig 1. Model with homogeneous risk. (A) Age-specific malaria incidence data (red circles) and the best fitting model output (blue line). (B) Frequency distribution of the number of cases per person, empirical data (red bars) and model output (blue bars). (C) Homogeneous risk distribution. (D) Age-dependent force of infection (Equation 1) with parameters $\lambda_0 = 0.7452$, $c = 0.8787$ and $k = 0.0282$. (E) Partial immunity factor (Equation 2) with parameter $\alpha = 0.1162$.

A 20% fraction of high-risk individuals accounts for 86% of the community-wide malaria burden

We next consider two susceptibility classes (high-risk [HR] and low-risk [LR] groups) to account for risk heterogeneity in the host population. We optimised model fitting (S1 File) for different

proportions of individuals in the HR and LR groups, with the best fit corresponding to a model with 20% of the host population allocated to the HR group (Table 1).

Table 1. Model fitting for different risk distributions

HR-LR (in %)	Log-likelihood
0-100	118.4802
10-90	133.2681
15-85	141.4236
20-80	**142.6645**
25-75	140.6231
30-70	137.4449

The best-fitting solution obtained with the heterogeneous model is presented in Fig 2. Fig 2A compares empirical age-specific malaria incidence data to the model output, which combines incidence densities in the LR and HR groups. Overall, the HR group is estimated to contribute 86.0% of the overall vivax malaria burden in the community, roughly as expected from the "20/80 rule" [1]. High-risk individuals become infected earlier and acquire partial immunity faster than their low-risk counterparts, resulting in markedly different, subgroup-specific age-incidence patterns. In the HR group, the incidence of clinical malaria sharply increases with age among children and adolescents, but declines thereafter; in contrast, malaria incidence density increases slowly in the LR group and reaches a plateau in the fourth decade of life. Fig 2B shows that the model properly fits the empirical frequency distribution of cases per person accumulated over one year of follow-up.

144 **Fig 2. Model with heterogeneous risk.** (A) Age-stratified incidence data (red circles) and the
145 model output (blue line) as a composition of incidence densities in the low-risk (LR; red line)
146 and high-risk (HR; yellow) groups. (B) Frequency distribution of the number of cases per
147 person, empirical data (red bars) and model output (blue bars). (C) Risk distribution with
148 variance $v = 3.3247$ [95% credible interval: 3.1057 - 3.3845], partitioning the population into
149 80% ($p_1 = 0.8$) in the LR group ($x_1 = 0.0883$ [95% CI: 0.0801- 0.1189]) and 20% ($p_2 = 0.2$) in
150 the HR group ($x_2 = 4.6467$ [95% CI: 4.5246- 4.6794]). (D) Age-dependent force of infection
151 (Equation 1) with parameters $\lambda_0 = 0.6197$ [95% CI: 0.3680 - 0.7174], $c = 0.8720$ [95% CI:
152 0.6638 - 0.9642] and $k = 0.0493$ [95% CI: 0.0392 - 0.1173]. (E) Partial immunity factor
153 (Equation 2) with parameter $\alpha = 0.0285$ [95% CI: 0.0162 - 0.0330].
154
155 Figs 2C, 2D and 2E show, respectively, the risk distribution, the age-dependent force of
156 infection and the partial immunity factor. The risk distribution has variance $v = 3.3247$ [95%
157 credible interval: 3.1057 - 3.3845], with 80% ($p_1 = 0.8$) of the population having low risk $x_1 =$
158 0.0883 [95% CI: 0.0801- 0.1189]) (LR group) and 20% ($p_2 = 0.2$) high risk $x_2 = 4.6467$ [95%
159 CI: 4.5246- 4.6794]) (HR group). Note that *P. vivax* malaria risk is approximately 26-fold higher
160 in individuals in the $S_{0,2}$ compartment, which comprises malaria-naïve high-risk subjects,
161 compared to their counterparts in the $S_{0,1}$ compartment, which comprises malaria-naïve low-
162 risk subjects. However, this difference changes with age as individuals in each group become
163 infected and acquire partial immunity. The model fits the data optimally when the age-
164 dependent force of infection (Equation 1) takes parameter values $\lambda_0 = 0.6197$ [95% CI:
165 0.3680 - 0.7174], $c = 0.8720$ [95% CI: 0.6638 - 0.9642] and $k = 0.0493$ [95% CI: 0.0392 -
166 0.1173], and the partial immunity factor (Equation 2) decays at rate $\alpha = 0.0285$ per infection
167 [95% CI: 0.0162 - 0.0330].

High-risk individuals develop immunity and constitute a clinically silent reservoir of infection

We next incorporate to the model, compartments with individuals who are infected but asymptomatic. The dynamics of individuals through model compartments, considering that asymptomatic infections last an average of 90 days (i.e. γ'= 1/90 per day), is shown in Fig 3. Individuals in the LR group move slowly between compartments (Fig 3A, 3B and 3C), compared with their HR counterparts (Fig 3D, 3E and 3F). Using the population age structure determined by our census survey, the model predicts that, in the current population, 77.8% and 5.4% of the individuals of the HR and LR groups, respectively, had at least one clinical malaria attack. As a consequence, acquired immunity following repeated *P. vivax* malaria episodes affects almost exclusively the dynamics of HR individuals, leading to frequent asymptomatic infections (Figs 3C and 3F).

Fig 3. Age-profiles of repeated malaria in a heterogeneous host population comprising a high-risk (HR) and a low-risk (LR) group. (A) Susceptible individuals in the LR group; (B) Symptomatic infected individuals in the LR group; (C) Asymptomatic individuals in the LR group; (D) Susceptible individuals in the HR group; (E) Symptomatic infected individuals in the HR group; (F) Asymptomatic individuals in the HR group.

Because the asymptomatic infection recovery rate γ' is unknown, we assumed the average duration of asymptomatic parasite carriage (D_A) to range from 30 to 180 days (Fig 4). Model outputs recapitulate the age-dependent increase in the prevalence of asymptomatic *P. vivax*

191 carriage that has been described in Amazonian communities (Fig 4A; e.g., [21]) and, as
192 expected, indicate that the community-wide prevalence of asymptomatic *P. vivax* infection
193 increases with longer parasite carriage duration (Fig 4B). Model simulations indicate that HR
194 individuals constitute the vast majority of asymptomatic parasite carriers (Fig 4C). Although
195 this maybe somewhat overrated due to the assumption that acquired immunity reduces
196 symptoms without preventing infection, it highlights plausible trends warranting future
197 empirical studies.
198
199 **Fig 4. Prevalence of asymptomatic *Plasmodium vivax* infection according to the average**
200 **duration of parasite carriage.** (A) Age-stratified prevalence of asymptomatic infection
201 considering an average duration of asymptomatic parasite carriage D_A of 30, 90 and 180 days.
202 (B) Variation in the community-wide prevalence of asymptomatic infection according to the
203 average duration of asymptomatic parasite carriage. (C) Age-stratified prevalence of
204 asymptomatic infection in the low-risk (LR) and high-risk (HR) groups considering an average
205 duration of asymptomatic parasite carriage D_A of 30 days (upper panel), 90 days (middle panel)
206 or 180 days (lower panel).
207
208 The relative contribution of asymptomatic and symptomatic infections to the overall burden
209 of *P. vivax* infection in the community was also simulated (Fig 5). We observe that, even with
210 short-lived asymptomatic parasite carriage ($D_A = 1/\gamma' = 30$ days) and considering the
211 average duration of symptomatic infections that are diagnosed and treated as either 4, 8, or
212 12 days, 66-85% of subjects carrying *P. vivax* infection at a given time will be asymptomatic,
213 consistent with empirical estimates from across the Amazon ranging between 52% and 90%

[21-24]. We note that these empirical data can be used to estimate γ' and D_A in the target populations.

Fig 5. Simulated proportions of community-wide *Plasmodium vivax* infections that are symptomatic or asymptomatic. We consider the average duration of symptomatic infections that are diagnosed and treated as either 4, 8, or 12 days; the duration of asymptomatic parasite carriage that remains undetected and untreated (D_A) is considered to be 30 days (panel A), 90 days (panel B), or 180 days (panel C).

Finally, we simulated the relative contribution of asymptomatic parasite carriers to onwards *P. vivax* transmission in a wide range of plausible scenarios. To this end, we consider that symptomatic and asymptomatic parasite carriers remain infectious for 4, 8 and 12 days and 30, 90 and 180 days, respectively, with a relative infectiousness (*RI*) of asymptomatic compared to symptomatic infections of 1/2, 1/10 and 1/30 (Fig 6). Model outputs indicate that even short-lived asymptomatic *P. vivax* carriage ($D_A = 30$ days) can contribute substantially to onwards malaria transmission in the community if the overall *RI* ranges between 1/2 and 1/10 (Figs 6A and 6D). Sustained asymptomatic *P. vivax* carriage ($D_A = 90$ days) can account for 30-87% of the infectious reservoir if *IR* ranges between 1/2 and 1/10 (Figs 6B and 6E), with a minor further increase with $D_A = 180$ days (Figs 6C and 6F). We further note that, for most D_A and *RI* value combinations, the relative contribution of symptomatic infections to the infectious reservoir can be substantially reduced by providing prompt CQ-PQ treatment to reduce the mean gametocyte clearance time (or average duration of infectiousness) from 12 to 4 days.

Fig 6. Relative contribution to the *Plasmodium vivax* infectious reservoir of individuals with symptomatic and asymptomatic infections. Model outputs consider different average durations of asymptomatic parasite carriage D_A ($D_A = 30$ days in panels A, D and G; 90 days in panels B, E and H; and 180 days in panels C, F and I) and different relative infectiousness (*RI*) of asymptomatic compared to symptomatic infections (*RI* = 1/2 in panels A, B and C; 1/10 in panels D, E and F; and 1/30 in panels G, H and I. For every combination of D_A and *RI*, we simulated the average duration of infectiousness of symptomatic infections as either 4, 8 or 12 days.

Discussion

Measuring how malaria infection risk varies among individuals is challenging. Product of exposure to infectious mosquitoes and susceptibility to infection given exposure, each individual's risk is determined by numerous interacting factors. Despites notorious efforts being invested in characterising specific determinants, such as individual mobility to and from hotspots [25], parasite genetics [26] and human genetics [27], a complete catalogue of risk factors and respective measures is not on the horizon. Smith [28] suggested that individual-level variation in susceptibility to malaria given exposure can be inferred by modelling malaria incidence as a function of EIR measured in the same population. Similarly, matched EIR and parasite prevalence data have been used to quantify heterogeneity in malaria susceptibility by assuming a gamma distribution of relative infection rates in the host population [5]. However, the widespread use of these approaches is limited by the restricted availability of reliable EIR measurements, which are notoriously difficult to obtain, from across endemic communities. Malaria transmission models that consider heterogeneity have instead assumed either a small

number of measured risk factors or unmeasured ranges of individual risk variation incorporated as either discrete frailty groups or a continuous variable (e.g., [29]).

Here, we show that a compartmental SIS model with heterogeneous risk notoriously outperforms its mean-field approximation in recapitulating the transmission dynamics of *P. vivax* in the main malaria hotspot of Brazil. We provide an empirical basis to estimate risk heterogeneity in host populations by simultaneously fitting SIS models to two sets of surveillance data -- namely, age-related malaria incidence and frequency distribution of malaria cases per person -- derived from the same population-based cohort. The best-fitting heterogeneous-risk model considers that the HR group comprises 20% of the host population and contributes 86% of the vivax malaria burden in the community. We suggest that this approach can be used to fit empirical data from across a range of malaria-endemic settings to test whether other host populations conform to this 20/80 pattern.

The estimated force of infection in the main residual malaria hotspot of Brazil is one order of magnitude lower than that estimated for *P. falciparum* in children from across rural Africa (e.g., [20, 30]). As a consequence, our study population appears to acquire partial immunity to malaria rather slowly. Indeed, the model predicts that as much as 25 past clinical malaria attacks, on average, are required in order to reduce by half the risk of a clinical malaria attack. In holoendemic settings, children are typically continuously infected during the transmission season, with frequent superinfection and overlapping clinical malaria episodes during their first years of life. For example, children aged 1-5 years in Papua New Guinea were estimated to experience an average of 2.5 episodes of clinical vivax malaria per year in 2006-2007, before intensified, large-scale control interventions were implemented nationwide [31]. Similarly, in

Mali an average of 2.4 episodes of clinical falciparum malaria per child aged 3-59 months per year have been estimated to occur, despite the distribution of long-lasting insecticide-treat bed nets at baseline [32]. Both estimates give an average of 25 malaria attacks by the age of 10-11 years. Indeed, in such areas, malaria remains common throughout most of childhood, and a significant decrease in risk of infection is seen in adolescence and early adulthood. In our study site, although partial immunity develops earlier in the HR group, with a decline in malaria incidence after the second decade of life (Fig 2A), HR individuals across all age groups still constitute the main contributors to the overall clinical malaria burden.

Despite the low overall force of infection in the study area, the fraction of HR individuals who experience repeated *P. vivax* infections and gradually develop partial immunity will eventually become asymptomatic but potentially infectious parasite carriers overlooked by routine surveillance. Although the overall average incidence of clinical *P. vivax* malaria in Mâncio Lima, estimated at 20.90 episodes/100 person-years at risk between October 2015 and September 2016, is substantially lower than that observed in holoendemic settings, some HR individuals may be nearly as exposed to malaria as the average child living in rural Africa. In fact, around one fourth of study subjects experienced one or more episodes of clinical vivax malaria during the study period; 29.9% of those with symptomatic *P. vivax* infections diagnosed during the study period had two or more episodes (Fig 2B, red bars), indicating that a fraction of exposed subjects actually experience repeated *P. vivax* episodes over one year of follow-up. Therefore, the paradoxical finding of clinical immunity and frequent asymptomatic infections in Amazonian communities exposed to low overall levels of malaria transmission [33] can be explained by the presence of a fraction of HR subjects that experience the majority of infections in the community and acquire clinical immunity. Statistical modelling of malaria

surveillance data has identified young adult males living in the less urbanized periphery of the town as the main HR individuals in Mâncio Lima [34]. Importantly, these HR individuals not only contribute disproportionately to the overall burden of clinical disease (Fig 2A), but also constitute the silent reservoir of sustained asymptomatic infections (Fig 4C) that are left untreated and may contribute significantly to onwards malaria transmission in this and other low-endemicity settings [35]. Estimates of the proportions of asymptomatic infections that are patent (consistent with *RI* close to 1/2) vary by one order of magnitude, from 4.5% [24] to 46.7% [22], in Amazonian populations.

The importance of characterising malaria reservoirs in endemic regions has recently been highlighted [36] and the results from this work further underscore how essential this information is to inform elimination programmes for properly planning control interventions. Heterogeneous risk implies that imperfect control measures, such as leaky vaccines, if uniformly applied to the entire host population, are unlikely to reduce substantially the overall malaria burden [29]. Our model simulations, however, suggest that a dramatic reduction in the community-level burden of clinical *P. vivax* malaria can be achieved by selectively targeting HR subjects, if they can be readily identified, to more intensive and effective measures that may not be readily delivered to the entire population.

We have limited the present analysis to *P. vivax*, which predominates in the areas of residual malaria transmission across the Amazon Basin. One major feature of *P. vivax* is that parasites may persist for several months in human hosts as hypnozoites, the dormant liver stages that eventually reactivate and may cause one or more new blood-stage infections termed relapses following a single infectious mosquito bite [37]. Radical cure of vivax malaria thus requires the

use of antimalarial drugs that target both blood and liver stages, such as PQ and tafenoquine. Although we do not consider relapses explicitly in our compartmental models, they are implicitly integrated into the force of infection, which combines blood-stage infections arising from infecting stages (sporozoites) inoculated during mosquito bites and relapses arising from reactivating hypnozoites. We hypothesise that HR and LR individuals initially differ in their exposure to infectious mosquitoes or susceptibility to infection and disease once challenged with infecting sporozoites, but over time HR individuals become also more likely to have *P. vivax* relapses originating from the large hypnozoite reservoir that they have accumulated in the liver following repeated infections. Importantly, new infections and relapses entail different control measures; while the incidence of new infections can be reduced by decreasing exposure to mosquito bites, e.g. with insecticide-treated bednets, relapses can be prevented by improved anti-relapse treatments.

The present study has some limitations. First, we used routinely collected malaria morbidity data for model fitting, but blood samples were not available for further confirmatory (e.g., molecular) diagnostic tests. Moreover, surveillance data used to fit our models do not include sub-patent and asymptomatic malaria episodes experienced by the target population. Second, our modelling approach does not allow for estimating the impact of improved anti-relapse therapies on the overall *P. vivax* malaria burden, since we do not differentiate between blood-stage infections arising from hypnozoites and newly inoculated sporozoites. Third, there are no empirical data, obtained in the same population, to properly measure the relative infectiousness of asymptomatic infections, either patent or not, and estimate more precisely their potential contribution to malaria transmission in the community.

Materials and Methods

Ethics statement

The study protocol was approved by the Institutional Review Board of the Institute of Biomedical Sciences, University of São Paulo, Brazil (CEPH-ICB 1368/17); written informed consent and assent were obtained for the census survey.

Study site and population

The study site, the municipality of Mâncio Lima (07°36' 51"S, 72°53' 45"W), is situated in the upper Juruá Valley, next to the border between Brazil and Peru. With 17,910 inhabitants (half of them in the urban area) and 9,278 laboratory-confirmed malaria cases notified in 2017, Mâncio Lima has currently the highest annual parasite incidence (API) in Brazil, estimated at 518.0 malaria cases per 1,000 inhabitants. Mâncio Lima is unique in Brazil in that 49% of all local malaria infections are reportedly acquired in urban settings, compared to a country's average of 15% (Ministry of Health of Brazil; unpublished data available at: http://www.acessoainformacao.gov.br/).

The study cohort comprised 8,783 permanent residents in the town of Mâncio Lima, aged from <1 to 80 years and distributed into 2,329 households. These individuals were systematically enumerated during a demographic census survey carried out by our field team between November 2015 and April 2016. Dates of entry in the study cohort were the subject's date of birth or October 1, 2015, whatever was the most recent; this information was used to calculate the number of person-years at risk for incidence density estimation. For the purposes of this

analysis, we assumed that no study participant left the study area before September 30, 2016, when the latest morbidity data were collected.

Malaria morbidity data

We retrieved all records of laboratory-confirmed clinical malaria cases notified in Mâncio Lima between October 1, 2015, to September 30, 2016. Case records were entered into the electronic malaria notification system of the Ministry of Health of Brazil (SIVEP-Malaria; http://200.214.130.44/sivep_malaria/). Because malaria is a notifiable disease in Brazil and only public health facilities provide laboratory diagnosis and malaria treatment, the electronic malaria notification system is estimated to comprise 99.6% of all clinical malaria cases diagnosed countrywide [38]. However, asymptomatic parasite carriage and persistently subpatent infections, which are not detected by microscopy or commercially available, antigen-based rapid diagnostic tests, may have been overlooked. We used patient's name, gender, and age to link malaria case records to individuals in our census survey database, given the absence of common unique patient identifiers. Name entries were compared using the Jaro-Winkler string distance [39] as implemented in the *stringdist* package of the *R* software [40]. Criteria for associating malaria case records to subjects enumerated during our census survey were: (a) same gender, (b) maximum reported age difference of 1 year, and (c) maximum Jaro-Winkler distance between names of 0.10, with penalty factor of 0.05 (constant scaling factor for how much the score is adjusted downwards for having common prefixes).

A minimal interval of 28 days between two consecutive malaria notifications was required to count the second case as a new malaria episode. When different infecting species were

401 detected in samples obtained less than 28 days apart, the subject was considered to have a
402 single mixed-species infection. Overall, we found 2,057 malaria notifications in the cohort of
403 urban residents during the 12-month study period, with 8,770.8 person-years of follow-up. *P.*
404 *vivax* accounted for 1,833 cases (89.1%), *P. falciparum* for 193 cases (9.4%) and both species
405 for 31 cases (1.5%). The present analysis is limited to *P. vivax* infections, since this is the most
406 abundant in our study location. Describing the transmission dynamics of multiple *Plasmodium*
407 species would escalate model complexity and assumptions beyond the realm of the current
408 study. We found an average malaria vivax incidence density of 20.90 episodes/100 person-
409 years at risk. By combining demographic information and malaria morbidity data, we
410 computed age-specific vivax malaria incidence densities and the number of vivax malaria
411 episodes per person recorded in the urban cohort over 12 months. These empirical data were
412 used to fit model outputs.
413

414 The mathematical model

415 The compartmental SIS model describing the epidemiology of clinical vivax malaria is
416 represented diagrammatically in Fig 7. Any population of susceptible individuals is
417 heterogeneous with regards to risk of infection. Individual risk is a continuous characteristic
418 which we discretise in two groups: low risk (LR) and high risk (HR). This is a coarse description
419 of individual heterogeneity that nevertheless suffices to our modelling purposes of capturing
420 the effects of variance in risk. Within each risk group, individuals are classified as either
421 susceptible or infected. Each risk group comprises a proportion p_j ($0 < p_j < 1,\ j = 1, 2$ and
422 $p_1 + p_2 = 1$) of the total population and is associated with a risk factor $x_j > 0$ ($j = 1, 2$).
423 Without loss of generality, we assume that the overall average risk is equal to 1 ($x_1 p_1 + x_2 p_2 =$

1) since the factors x_j are modifiers of individual responses to a force of infection which will be allowed to vary. This setting configures a risk distribution with variance $v = p_1(x_1 - 1)^2 + p_2(x_2 - 1)^2$.

Fig 7. Susceptible-infected-susceptible (SIS) compartmental model representing the dynamics of malaria over age in a heterogeneous host population. The compartments describe the following epidemiological classes: $S_{i,j}$ represents susceptible individuals from risk group j (1 = low-risk [LR]; 2 = high-risk [HR]) who have experienced i past clinical malaria attacks; $I_{i,j}$ represents symptomatic infected individuals from risk group j who are currently experiencing their ith clinical malaria attack. Individuals experience new infections due to an age-dependent force of infection $\lambda(a)$ modified by a risk factor x_j, and a partial immunity weight $\sigma(i)$; all individuals recover at the same rate γ.

We assume an age-dependent force of infection $\lambda(a)$ (Equation 1), which correlates mosquito biting activity with human body mass [30, 41]. This function strictly increases with age, with minimum $\lambda_0(1 - c)$ (at age zero) and upper limit λ_0. The parameter k determines how steeply the force of infection increases in early ages and c controls the value at birth.

$$\lambda(a) = \lambda_0(1 - ce^{-ka}) \quad (1)$$

Assuming that individuals acquire partial immunity after repeated clinical malaria attacks, due to antibody- and cell-mediated responses [42], we introduce a factor describing the development of partial immunity. The strictly positive decreasing function $\sigma(i)$ of the number i ($i \geq 0$) of past clinical vivax malaria attacks each individual has experienced (Equation 2), with

a maximum for malaria-naïve individuals ($\sigma(0) = 1$), simulates a partial immunity factor and weights down the age-dependent force of infection $\lambda(a)$ as the number of cumulative clinical malaria episodes increases. The factor describing partial immunity is controlled by the parameter α, which determines the rate at which immunity develops after repeated infections.

$$\sigma(i) = e^{-\alpha \cdot i} \tag{2}$$

Assuming equilibrium with respect to time, in addition to the age-dependent force of infection, partial immunity acquisition and risk heterogeneity, malaria unfolds in age domain according to a system of ordinary differential equations (ODEs) (system of equations 3).

$$\begin{aligned}
\frac{dS_{0,j}}{da} &= -x_j\sigma(1)\lambda(a)S_{0,j} \\
\frac{dI_{1,j}}{da} &= +x_j\sigma(1)\lambda(a)S_{0,j} - \gamma I_{1,j} \\
\frac{dS_{1,j}}{da} &= -x_j\sigma(2)\lambda(a)S_{1,j} + \gamma I_{1,j} \\
\frac{dI_{2,j}}{da} &= +x_j\sigma(2)\lambda(a)S_{1,j} - \gamma I_{2,j} \\
&\vdots \\
\frac{dS_{n-1,j}}{da} &= -x_j\sigma(n)\lambda(a)S_{n-1,j} + \gamma I_{n-1,j} \\
\frac{dI_{n,j}}{da} &= +x_j\sigma(n)\lambda(a)S_{n-1,j} - \gamma I_{n,j} \\
&\vdots
\end{aligned} \qquad \begin{aligned}
&\text{Initial conditions:} \\
&S_{0,j}(0) = p_j \\
&S_{i,j}(0) = I_{i,j}(0) = 0 \\
&j = 1,2\ ,\ i = 1,2,\ldots
\end{aligned} \tag{3}$$

Individuals in the LR group are initially allocated to compartment $S_{0,1}$, comprising susceptible individuals who are malaria-naïve. At a rate which is determined by the age-dependent force of infection $\lambda(a)$ and the risk factor x_1, LR individuals move to compartment $I_{1,1}$ after experiencing their first clinical vivax malaria attack. After recovering (with recovery rate γ),

462 they become susceptible again and move to the next compartment $S_{1,1}$, which comprises
463 susceptible individuals who have already experienced one past malaria attack and acquired
464 some degree of partial immunity. These individuals may acquire a second infection, according
465 to the same age-dependent force of infection and risk factor, but now weighted down by the
466 partial immunity $\sigma(1)$. LR individuals can move forward between compartments within the LR
467 group. With similar dynamics, HR individuals move forward within the HR group, but with a risk
468 factor x_2 (Fig 7). This is denominated as the heterogeneous risk model.
469
470 For comparison purposes, we built a similar compartmental model where the same average
471 risk is applied to the entire host population (homogeneous risk model; $p_1 = 1$ and $x_1 = 1$, e.g.,
472 [20]). We fitted the heterogeneous and the homogeneous risk models to empirical data and
473 compared their ability to recapitulate the epidemiology of vivax malaria in the study
474 population.
475

476 Mathematical model with asymptomatic infections

477 We refined the SIS model with compartments comprising infected but asymptomatic
478 individuals, by assuming that the proportion of asymptomatic infections depends on gradually
479 acquired partial immunity. This partial immunity is sometimes termed "clinical" or "anti-
480 disease immunity" to emphasise that individuals remain susceptible to infection but become
481 gradually less likely to develop clinical disease once infected. We followed the same basic
482 assumptions of the first model: susceptible individuals from risk group j, with age a and with i
483 past clinical attacks ($S_{i,j}(a)$) develop their ith clinical case at rate $x_j\sigma(i)\lambda(a)$. Partial immunity
484 developed after i past attacks (Equation 2) reduces by $1 - \sigma(i)$ the probability of susceptible

485 individuals $S_{i,j}(a)$ presenting clinical symptoms once infected again. Note that in this model
486 rates of clinical malaria episodes decline explicitly due to clinical immunity, in contrast with the
487 previous implementation which did not specify whether these declines were due to immunity
488 against disease or against infection. Infected subjects thus move to the asymptomatic
489 compartment A if they do not develop clinical malaria upon infection. More formally,
490 susceptible individuals $S_{i,j}(a)$ become infected but asymptomatic $A_{i,j}(a)$ at rate $x_j(1 -$
491 $\sigma(i))\lambda(a)$. Individuals with asymptomatic infections from group j, age a and who experienced
492 i past clinical malaria attacks ($A_{i,j}(a)$) can eventually progress to their ith new clinical attack,
493 at rate $x_j\sigma(i)\lambda(a)$, or recover and become susceptible again at rate γ'. The compartmental
494 SIS model considering asymptomatic infections is represented diagrammatically in Fig 8.
495
496 **Fig 8. Susceptible-infected-susceptible (SIS) compartmental model representing the dynamics**
497 **of malaria in a heterogeneous host population considering asymptomatic infections.** The
498 compartments correspond to the following epidemiological classes: $S_{i,j}$ represents susceptible
499 individuals from risk group j (1 = low-risk [LR]; 2 = high-risk [HR]) who have experienced i
500 clinical malaria attacks; $I_{i,j}$ represents individuals with symptomatic infection from risk group
501 j who are currently experiencing their ith clinical malaria attack; $A_{i,j}$ represents individuals
502 with asymptomatic infections from risk group j with i past clinical malaria attacks. Individuals
503 experience malaria episodes due to an age-dependent force of infection $\lambda(a)$ modified by a
504 risk factor x_j, and a partial immunity weight $\sigma(i)$. Individuals from compartments I and A
505 recover and become susceptible again at rates γ and γ', respectively.
506

We assume that naïve individuals from compartment $S_{0,j}(a)$ cannot remain asymptomatic once infected for the first time, since they have not yet developed partial immunity. Indeed, with acquired immunity modelled by an exponential function (Equation 2), we have for naïve individuals $\sigma(0) = 1$. Therefore, the probability of naïve individuals becoming infected but asymptomatic is 0 ($x_j . 0 . \lambda(a)$).

Introducing asymptomatic compartments (A) to the model does not change the dynamics of symptomatic infections, which are represented by our empirical morbidity data. With the assumptions describe above, both susceptible and infected but asymptomatic individuals are at risk of symptomatic infection; therefore, the incidence of clinical malaria and the frequency distribution of clinical cases per person remain the same for both models. We thus apply the same parameters estimated in the first model (parameter estimation process is fully described in S1 File), but can now distinguish uninfected and susceptible individuals from those who are infected but remain asymptomatic, according to the recovery rate γ'.

Asymptomatic parasite carriers, duration of infection and the infectious reservoir

We simulated several scenarios to address the relative contribution of asymptomatic parasite carriers to the overall burden of infection and onwards transmission in the community. First, we assume individuals with asymptomatic infections to be 2, 10 and 30 times less infectious to mosquitoes than individuals with symptomatic infections (relative infectiousness (*RI*) of 1/2, 1/10 and 1/30, respectively). Empirical *RI* estimates vary widely according to the average gametocyte density [43] and are close to 1/2 for microscopy-detected asymptomatic *P. vivax*

infections in Ethiopia [44] but range from 1/14 to 1/29 for asymptomatic infections in Colombia and Brazil that can be detected only by molecular methods [45, 46].

Next, we assume that, on average, symptomatic infections can be detected by laboratory methods during 4, 8 and 12 days. Symptomatic infections are curtailed by treatment and their average length primarily depends on: (a) the duration of the patent but subclinical period that precedes full-blown disease manifestations, which remains elusive; (b) the mean time from the appearance of symptoms to the introduction of chloroquine (CQ)-primaquine (PQ) treatment (2.7 days in our population [47]), and (c) the mean *P. vivax* clearance time following CQ-PQ treatment (1.9 day in our population; [47]). We thus divided the proportion of individuals within the infected (*I*) compartments by 7 (=28/4), 3.5 (28/8) or 2.3 (28/12) to represent the prevalence of symptomatic blood-stage infections that can be detected by laboratory methods during the subject's 28-day stay in the *I* compartments.

We further assume that asymptomatic blood-stage infections undetected by routine surveillance and left untreated can last between 30 and 180 days. Empirical evidence is rather limited in this area and the duration is clearly context-specific. Once detected by microscopy, asymptomatic *P. vivax* infections in 4 years-old Papua New Guinean children lasted on average 15 days [48], but the time elapsed *before* blood-stage parasite detection has not been measured. If asymptomatic *P. vivax* infections were first sampled at a random time point during their trajectory, the time to parasite clearance after detection (15 days) is expected to equal, on average, the time elapsed before parasite detection, giving a total duration of 30 days. Here we simulate scenarios with asymptomatic *P. vivax* infections between 30 and 180 days, which

553 corresponds to the median duration of asymptomatic *P. vivax* infections in a cohort study in
554 Vietnam [49].
555
556 Finally, we consider the duration of infectiousness to equal the total duration of blood-stage
557 infection in both symptomatic and asymptomatic carriers, under the assumption that virtually
558 all blood-stage *P. vivax* infections comprise mature gametocytes [22,50]. Empirical data from
559 Brazil show that vivax malaria patients become little infectious within 10 hours of CQ-PQ
560 treatment [51], but untreated asymptomatic carriers of subpatent *P. vivax* parasitemia may
561 remain infectious for up to 2 months after parasite detection [52].
562
563 We conclude that considering risk heterogeneity in the host population is crucial for properly
564 describing the transmission dynamics of *P. vivax* using compartmental SIS models and provide
565 a framework to test the hypothesis that a few HR subjects contribute the vast majority of the
566 vivax malaria burden at the community level. Moreover, HR subjects are important
567 contributors to the silent infectious reservoir that likely fuels onwards malaria transmission in
568 low-endemicity settings. These results can be further explored for the evidence-based
569 planning and deployment of control interventions towards the elimination of residual P. vivax
570 malaria across the Amazon Basin.
571

572 Acknowledgements

573 We thank Anaclara Pincelli, Odaílton A. Nery and Dr. Nathália F. Lima for carrying out field work,
574 Maria José Menezes for administrative support and Dr. Jan Hasenauer and Elba Raimundez

(Institute of Computational Biology, Helmholtz Zentrum München, München, Germany) for helpful discussions.

References

1. Woolhouse ME, Dye C, Etard JF, Smith T, Charlwood JD, Garnett GP, et al. Heterogeneities in the transmission of infectious agents: implications for the design of control programs. Proc Natl Acad Sci USA 1997;94:338-342.
2. Mwangi TW, Fegan G, Williams TN, Kinyanjui SM, Snow RW, Marsh K. Evidence for over-dispersion in the distribution of clinical malaria episodes in children. PLoS One. 2008;3:e2196.
3. Smith DL, Dushoff J, Snow RW, Hay SI. The entomological inoculation rate and *Plasmodium falciparum* infection in African children. Nature 2005;438:492-495.
4. Clark TD, Greenhouse B, Njama-Meya D, Nzarubara B, Maiteki-Sebuguzi C, Staedke SG, Seto E, Kamya MR, Rosenthal PJ, Dorsey G. Factors determining the heterogeneity of malaria incidence in children in Kampala, Uganda. J Infect Dis. 2008;198:393-400.
5. Wilson ML, Krogstad DJ, Arinaitwe E, Arevalo-Herrera M, Chery L, Ferreira MU, Ndiaye D, Mathanga DP, Eapen A. Urban malaria: Understanding its epidemiology, ecology, and transmission across seven diverse ICEMR network sites. Am J Trop Med Hyg. 2015;93(3 Suppl):110-123.
6. Mathanga DP, Tembo AK, Mzilahowa T, Bauleni A, Mtimaukenena K, Taylor TE, Valim C, Walker ED, Wilson ML. Patterns and determinants of malaria risk in urban and peri-urban areas of Blantyre, Malawi. Malar J. 2016;15:590.
7. Trape JF, Zoulani A. Malaria and urbanization in central Africa: the example of Brazzaville. Part II: Results of entomological surveys and epidemiological analysis. Trans R Soc Trop Med Hyg. 1987; 81 Suppl 2:10-8.

8. Kang SY, Battle KE, Gibson HS, Cooper LV, Maxwell K, Kamya M, *et al*. Heterogeneous exposure and hotspots for malaria vectors at three study sites in Uganda. Gates Open Res. 2018;2:32.
9. Rono J, Färnert A, Murungi L, Ojal J, Kamuyu G, Guleid F, et al. Multiple clinical episodes of *Plasmodium falciparum* malaria in a low transmission intensity setting: exposure versus immunity. BMC Med 2015;13:114.
10. Smith TA, Chitnis N, Penny M, Tanner M. Malaria modeling in the era of eradication. Cold Spring Harb Perspect Med 2017;7: a025460.
11. Dwyer G, Elkinton JS, Buonaccorsi JP. Host heterogeneity in susceptibility and disease dynamics: tests of a mathematical model. Am Nat. 1997;150:685-707.
12. Langwig KE, Wargo AR, Jones DR, Viss JR, Rutan BJ, Egan NA, et al. Vaccine effects on heterogeneity in susceptibility and implications for population health management. MBio 2017;8: pii: e00796-17.
13. King JG, Souto-Maior C, Sartori ML, Maciel-de-Freitas R, Gomes MGM. Variation in *Wolbachia* effects on *Aedes* mosquitoes as a determinant of invasiveness and vectorial capacity. *Nat Commun*. 2018; 9: 1483.
14. Coutinho FAB, Massad E, Lopez LR, Burattini MN, Struchiner CJ, Azevedo-Neto RS. Modeling heterogeneities in individual frailties in epidemic models. Math Comp Model 1999; 30: 97-115.
15. Katriel G. The size of epidemics in populations with heterogeneous susceptibility. J Math Biol 2012;65:237-262.
16. Hickson RI, Roberts MG. How population heterogeneity in susceptibility and infectivity influences epidemic dynamics. J Theor Biol 2014;350:70-80.
17. Gomes MGM, Oliveira JF, Bertolde A, Ayabina D, Nguyen TA, Maciel EL, et al. Introducing risk inequality metrics in tuberculosis policy development. *Nat Commun*. 2019;10: 2480.
18. Killeen GF. Characterizing, controlling and eliminating residual malaria transmission. Malar J. 2014;13:330.

19. Ferreira MU, Castro MC. Malaria situation in Latin America and the Caribbean: residual and resurgent transmission and challenges for control and elimination. Methods Mol Biol. 2019;2013:57-70.
20. Águas R, White LJ, Snow RW, Gomes MGM. Prospects for malaria eradication in sub-Saharan Africa. PLoS ONE 2008; 3: e1767.
21. Alves FP, Durlacher RR, Menezes MJ, Krieger H, Silva LH, Camargo EP. High prevalence of asymptomatic *Plasmodium vivax* and *Plasmodium falciparum* infections in native Amazonian populations. Am J Trop Med Hyg. 2002;66:641-648.
22. Barbosa S, Gozze AB, Lima NF, Batista CL, Bastos MS, Nicolete VC, et al. Epidemiology of disappearing *Plasmodium vivax* malaria: a case study in rural Amazonia. PLoS Negl Trop Dis. 2014;8:e3109.
23. Ladeia-Andrade S, Ferreira MU, de Carvalho ME, Curado I, Coura JR. Age-dependent acquisition of protective immunity to malaria in riverine populations of the Amazon Basin of Brazil. Am J Trop Med Hyg. 2009;80:452-459.
24. da Silva NS, da Silva-Nunes M, Malafronte RS, Menezes MJ, D'Arcadia RR, Komatsu NT, et al. Epidemiology and control of frontier malaria in Brazil: lessons from community-based studies in rural Amazonia. Trans R Soc Trop Med Hyg. 2010;104:343-350.
25. Wesolowski A, Eagle N, Tatem AJ, Smith DL, Noor AM, Snow RW, et al. Quantifying the impact of human mobility on malaria. Science 2012;338:267-270.
26. Chang HH, Wesolowski A, Sinha I, Jacob CG, Mahmud A, Uddin D, et al. Mapping imported malaria in Bangladesh using parasite genetic and human mobility data. eLife 2019;8:e4381.
27. Allison AC. Genetic control of resistance to human malaria. Curr Opin Immunol 2009;21:499–505.
28. Smith TA. Estimation of heterogeneity in malaria transmission by stochastic modeling of apparent deviations from mass action kinetics. Malar J 2008;7:12.

29. White MT, Griffin JT, Drakeley CJ, Ghani AC. Heterogeneity in malaria exposure and vaccine response: implications for the interpretation of vaccine efficacy trials. Malar J 2010;9:82.
30. Smith T, Killeen G, Lengeler C, Tanner M. Relationships between the outcome of *Plasmodium falciparum* infection and the intensity of transmission in Africa. Am J Trop Med Hyg 2004;71:80-86.
31. Ome-Kaius M, Kattenberg JH, Zaloumis S, Siba M, Kiniboro B, Jally S, et al. Differential impact of malaria control interventions on *P. falciparum* and *P. vivax* infections in young Papua New Guinean children. BMC Med. 2019;17:220.
32. Dicko A, Diallo AI, Tembine I, Dicko Y, Dara N, Sidibe Y, et al. Intermittent preventive treatment of malaria provides substantial protection against malaria in children already protected by an insecticide-treated bednet in Mali: a randomised, double-blind, placebo-controlled trial. PLoS Med. 2011;8:e1000407.
33. da Silva-Nunes M, Moreno M, Conn JE, Gamboa D, Abeles S, Vinetz JM, Ferreira MU. Amazonian malaria: asymptomatic human reservoirs, diagnostic challenges, environmentally driven changes in mosquito vector populations, and the mandate for sustainable control strategies. Acta Trop. 2012;121:281-291.
34. Corder RM, Paula GA, Pincelli A, Ferreira MU. Statistical modeling of surveillance data to identify correlates of urban malaria risk: A population-based study in the Amazon Basin. PLoS One. 2019;14:e0220980.
35. Lindblade KA, Steinhardt L, Samuels A, Kachur SP, Slutsker L. The silent threat: asymptomatic parasitemia and malaria transmission. Expert Rev Anti Infect Ther 2013;11:623-639.
36. Águas R, Maude RJ, Gomes MGM, White LJ, White NJ, Dondorp AM. Infectivity of chronic malaria infections and its consequences for control and elimination. *Clin Infect Dis* 2018;67:295-302.
37. White NJ, Imwong M. Relapse. Adv Parasitol. 2012;80:113-50.

38. Malaria: Case Monitoring in Brazil in 2014 [in Portuguese]. Available from: http://portalarquivos2.saude.gov.br/images/pdf/2015/agosto/18/2015-009---Mal--ria-para-publica----o.pdf
39. Winkler W. String comparator metrics and enhanced decision rules in the Fellegi-Sunter model of record linkage. American Statistical Association 1990 Proceedings of the Section on Survey Research Methods, pp. 354-359.
40. van der Loo MPJ. The stringdist package for approximate string matching. R Journal 2014; 6: 111-122.
41. Port GR, Boreham PFL, Bryan JH. The relationship of host size to feeding by mosquitos of the *Anopheles gambiae* Giles complex (Diptera, Culicidae). Bull. Entomol 1980;70:133-144.
42. Cowman AF, Healer J, Marapana D, Marsh K. Malaria: Biology and disease. Cell 2016;167:610-624.
43. Lin JT, Saunders DL, Meshnick SR. The role of submicroscopic parasitemia in malaria transmission: what is the evidence? Trends Parasitol. 2014 30:183-190.
44. Tadesse FG, Slater HC, Chali W, Teelen K, Lanke K, Belachew M, et al. The relative contribution of symptomatic and asymptomatic *Plasmodium vivax* and *Plasmodium falciparum* infections to the infectious reservoir in a low-endemic setting in Ethiopia. Clin Infect Dis. 2018;66:1883-1891.
45. Vallejo AF, García J, Amado-Garavito AB, Arévalo-Herrera M, Herrera S. *Plasmodium vivax* gametocyte infectivity in sub-microscopic infections. Malar J. 2016;15:48.
46. Martins-Campos KM, Kuehn A, Almeida A, Duarte APM, Sampaio VS, Rodriguez ÍC, et al. Infection of *Anopheles aquasalis* from symptomatic and asymptomatic *Plasmodium vivax* infections in Manaus, western Brazilian Amazon. Parasit Vectors. 2018;11:288.
47. Ladeia-Andrade S, Menezes MJ, de Sousa TN, Silvino ACR, de Carvalho JF Jr, Salla LC, et al. Monitoring the efficacy of chloroquine-primaquine therapy for uncomplicated *Plasmodium*

vivax malaria in the main transmission hot spot of Brazil. Antimicrob Agents Chemother. 2019;63:e01965-18.

48. Bruce MC, Donnelly CA, Packer M, Lagog M, Gibson N, Narara A, et al. Age- and species-specific duration of infection in asymptomatic malaria infections in Papua New Guinea. Parasitology. 2000;121:247-256.
49. Nguyen TN, von Seidlein L, Nguyen TV, Truong PN, Hung SD, Pham HT, et al. The persistence and oscillations of submicroscopic *Plasmodium falciparum* and *Plasmodium vivax* infections over time in Vietnam: an open cohort study. Lancet Infect Dis. 2018;18:565-572.
50. Lima NF, Bastos MS, Ferreira MU. *Plasmodium vivax*: reverse transcriptase real-time PCR for gametocyte detection and quantitation in clinical samples. Exp Parasitol. 2012;132:348-354.
51. Klein TA, Tada MS, Lima JB, Tang AT. Infection of *Anopheles darlingi* fed on patients infected with *Plasmodium vivax* before and during treatment with chloroquine plus primaquine in Costa Marques, Rondonia, Brazil. Mem Inst Oswaldo Cruz. 1992;87:191-195.
52. Alves FP, Gil LH, Marrelli MT, Ribolla PE, Camargo EP, da Silva LH. Asymptomatic carriers of *Plasmodium* spp. as infection source for malaria vector mosquitoes in the Brazilian Amazon. J Med Entomol. 2005;42:777-779.

Supporting information

S1 File. Parameter estimation process.

Abbreviations

720 API: annual parasite prevalence; CI: credible interval; CQ: chloroquine; EIR: entomological
721 inoculation rate; HR: high risk; LR: low risk; PQ: primaquine; SIS: susceptible-infected-
722 susceptible.

Figure 1

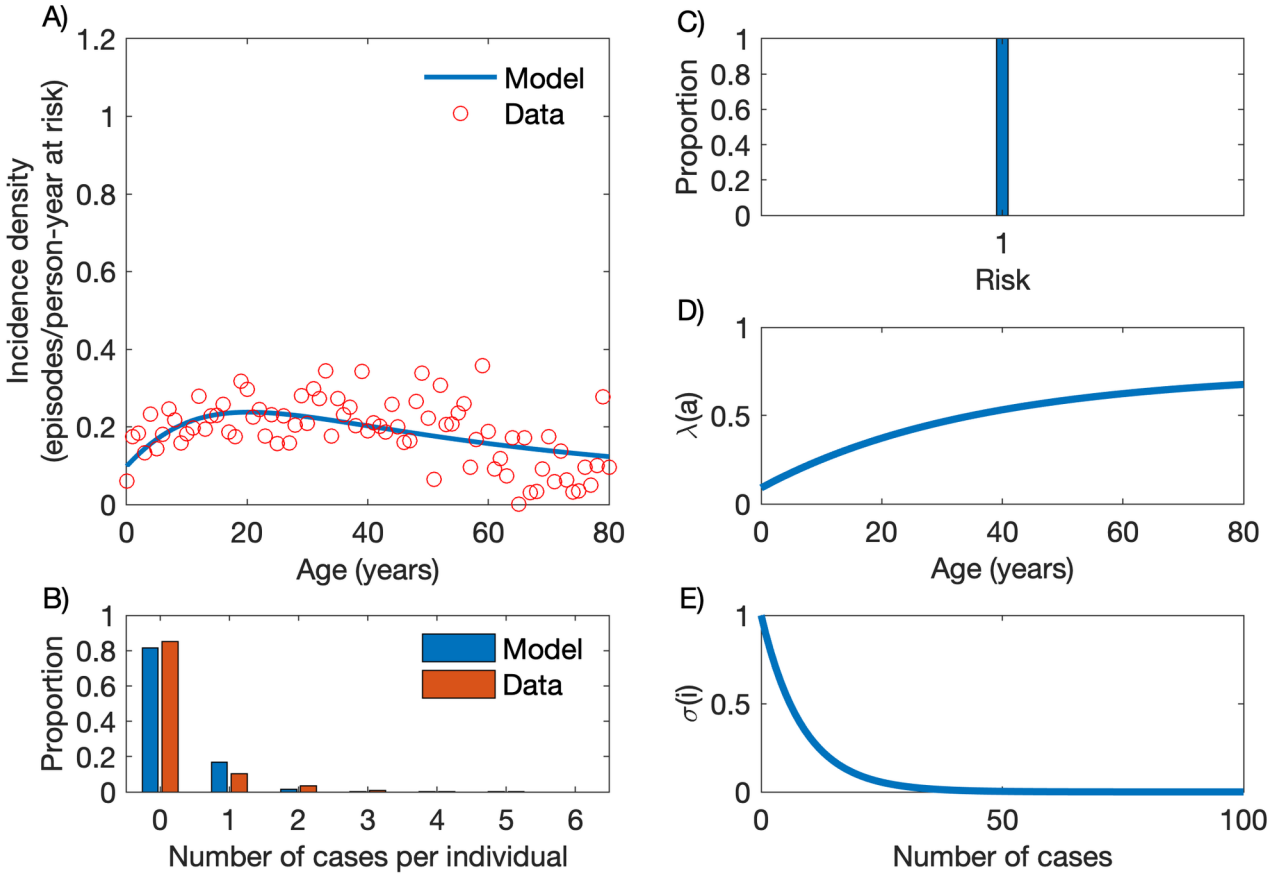
A)
Incidence density
(episodes/person-year at risk)
Model
Data
Age (years)
B)
Proportion
Model
Data
Number of cases per individual
C)
Proportion
Risk
D)
λ(a)
Age (years)
E)
σ(i)
Number of cases

Figure 2

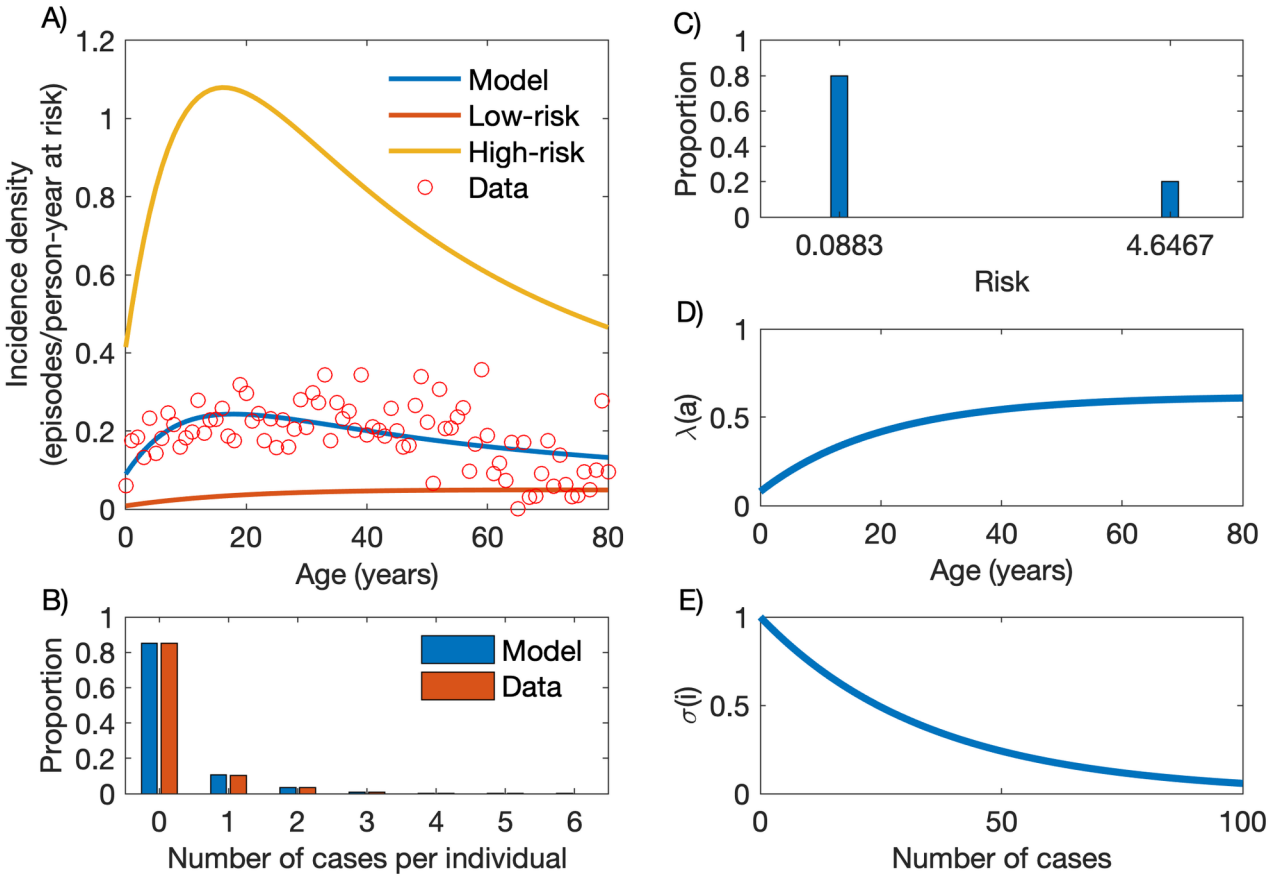
A)
Incidence density
(episodes/person-year at risk)
Model
Low-risk
High-risk
Data
Age (years)
B)
Proportion
Model
Data
Number of cases per individual
C)
Proportion
0.0883
4.6467
Risk
D)
λ(a)
Age (years)
E)
σ(i)
Number of cases

Figure 3

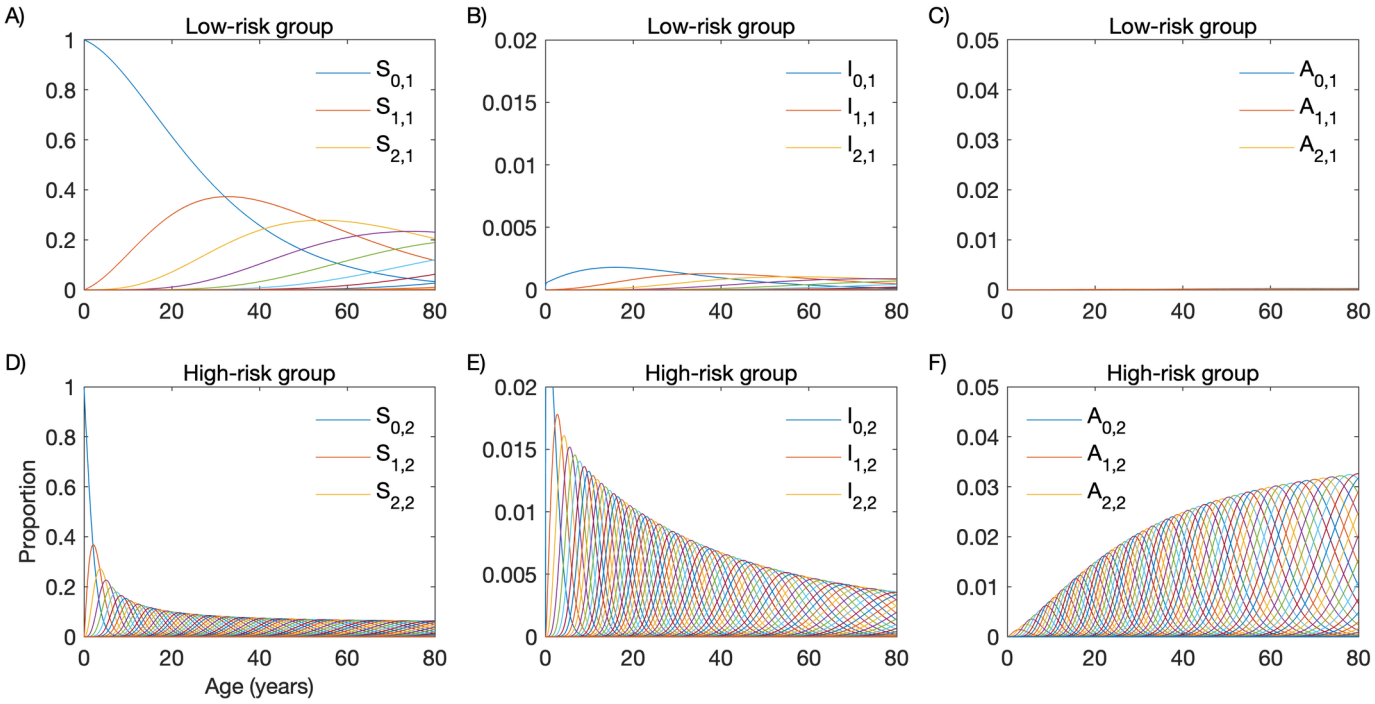
A)
Low-risk group
$S_{0,1}$
$S_{1,1}$
$S_{2,1}$
B)
Low-risk group
$I_{0,1}$
$I_{1,1}$
$I_{2,1}$
C)
Low-risk group
$A_{0,1}$
$A_{1,1}$
$A_{2,1}$
D)
High-risk group
$S_{0,2}$
$S_{1,2}$
$S_{2,2}$
Proportion
Age (years)
E)
High-risk group
$I_{0,2}$
$I_{1,2}$
$I_{2,2}$
F)
High-risk group
$A_{0,2}$
$A_{1,2}$
$A_{2,2}$

Figure 4

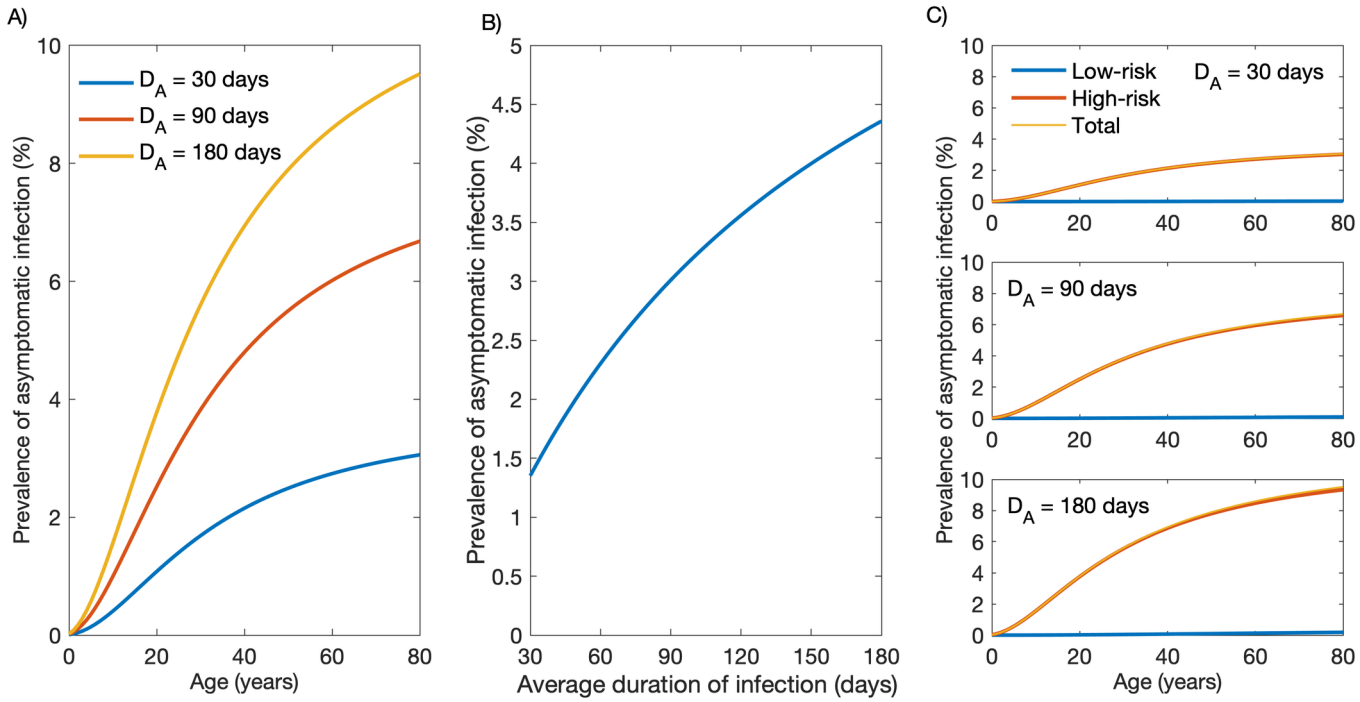
A)
B)
C)
Prevalence of asymptomatic infection (%)
Age (years)
D_A = 30 days
D_A = 90 days
D_A = 180 days
Average duration of infection (days)
Low-risk
High-risk
Total

Figure 5

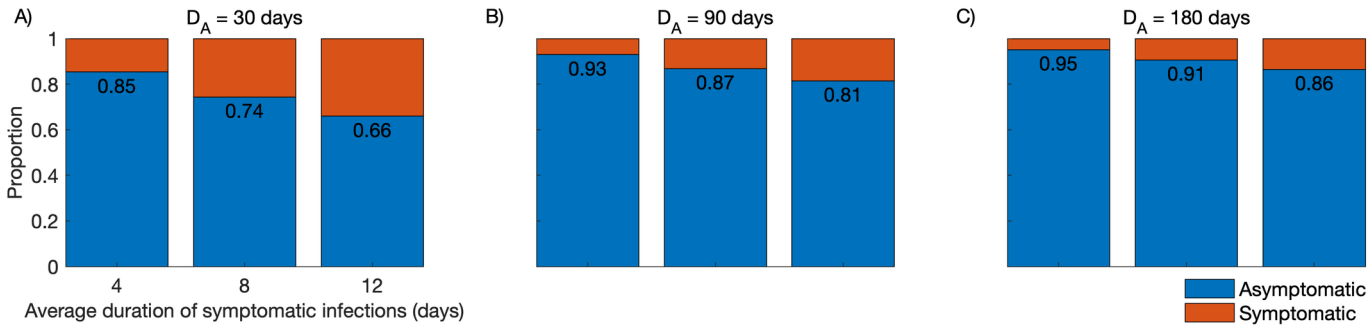
A)
D_A = 30 days
B)
D_A = 90 days
C)
D_A = 180 days
Proportion
1
0.8
0.6
0.4
0.2
0
0.85
0.74
0.66
0.93
0.87
0.81
0.95
0.91
0.86
4
8
12
Average duration of symptomatic infections (days)
Asymptomatic
Symptomatic

Figure 6

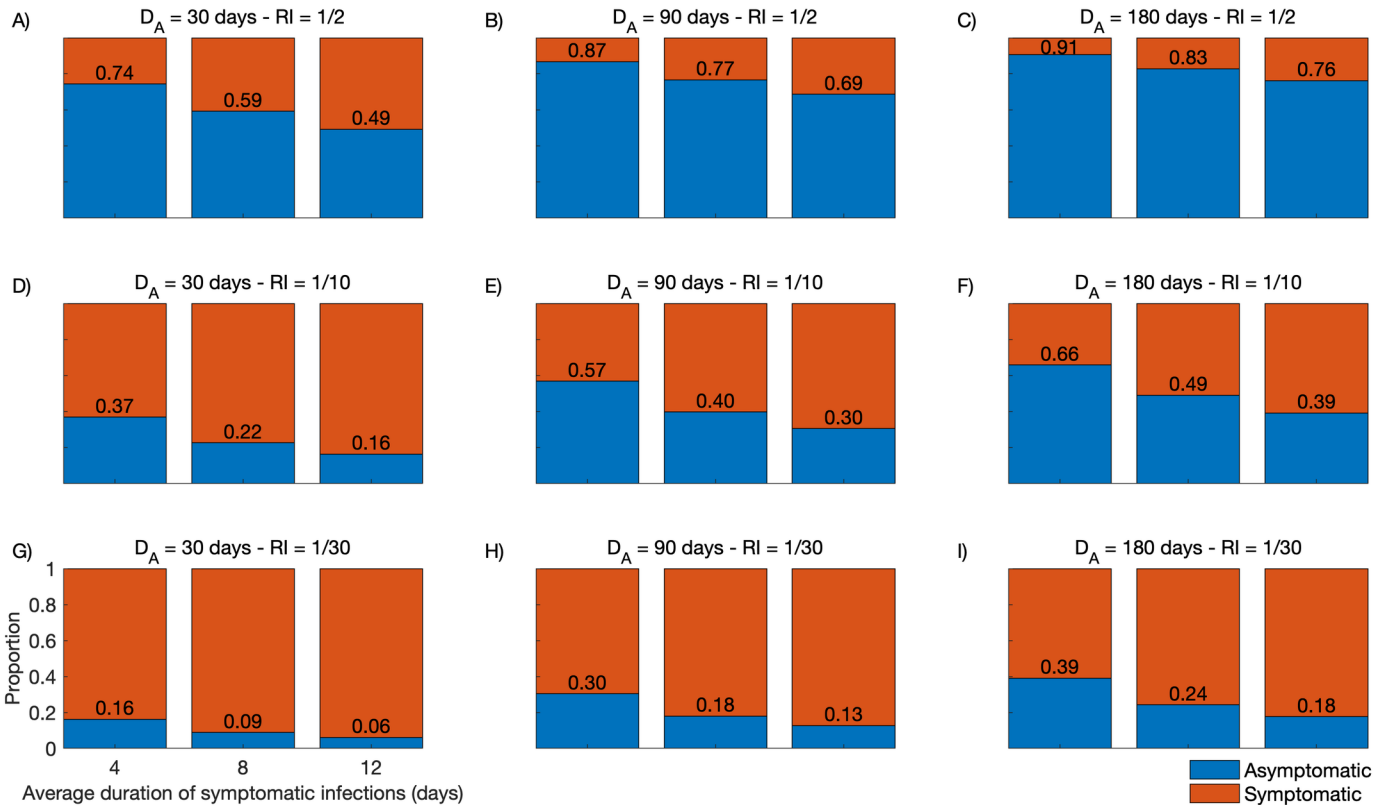
A)
D_A = 30 days - RI = 1/2
0.74
0.59
0.49
B)
D_A = 90 days - RI = 1/2
0.87
0.77
0.69
C)
D_A = 180 days - RI = 1/2
0.91
0.83
0.76
D)
D_A = 30 days - RI = 1/10
0.37
0.22
0.16
E)
D_A = 90 days - RI = 1/10
0.57
0.40
0.30
F)
D_A = 180 days - RI = 1/10
0.66
0.49
0.39
G)
D_A = 30 days - RI = 1/30
0.16
0.09
0.06
H)
D_A = 90 days - RI = 1/30
0.30
0.18
0.13
I)
D_A = 180 days - RI = 1/30
0.39
0.24
0.18
Proportion
0
0.2
0.4
0.6
0.8
1
4
8
12
Average duration of symptomatic infections (days)
Asymptomatic
Symptomatic

Figure 7

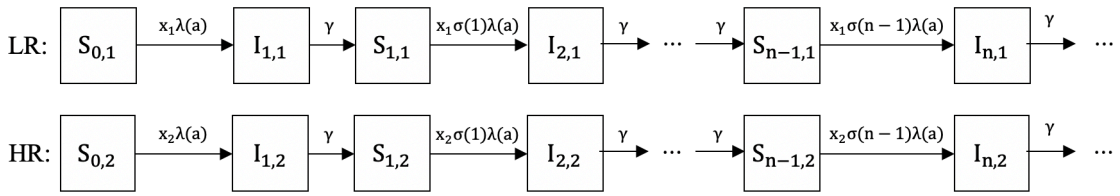
LR:
$S_{0,1}$
$x_1\lambda(a)$
$I_{1,1}$
γ
$S_{1,1}$
$x_1\sigma(1)\lambda(a)$
$I_{2,1}$
γ
$\cdots$
γ
$S_{n-1,1}$
$x_1\sigma(n-1)\lambda(a)$
$I_{n,1}$
γ
$\cdots$
HR:
$S_{0,2}$
$x_2\lambda(a)$
$I_{1,2}$
γ
$S_{1,2}$
$x_2\sigma(1)\lambda(a)$
$I_{2,2}$
γ
$\cdots$
γ
$S_{n-1,2}$
$x_2\sigma(n-1)\lambda(a)$
$I_{n,2}$
γ
$\cdots$

Figure 8

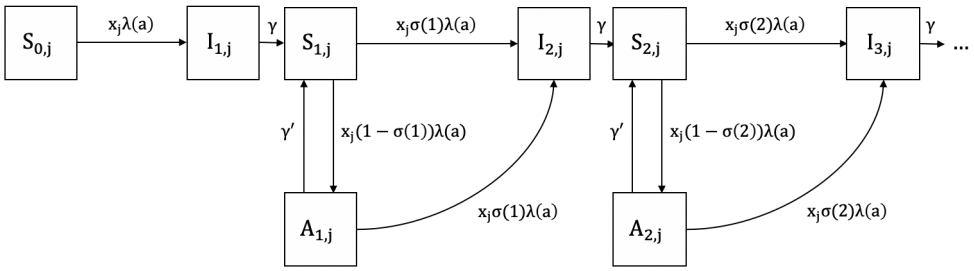
$S_{0,j}$
$x_j\lambda(a)$
$I_{1,j}$
γ
$S_{1,j}$
$x_j\sigma(1)\lambda(a)$
$I_{2,j}$
γ
$S_{2,j}$
$x_j\sigma(2)\lambda(a)$
$I_{3,j}$
γ
...
γ'
$x_j(1-\sigma(1))\lambda(a)$
$A_{1,j}$
$x_j\sigma(1)\lambda(a)$
γ'
$x_j(1-\sigma(2))\lambda(a)$
$A_{2,j}$
$x_j\sigma(2)\lambda(a)$

Parameter estimation process

The SIS compartmental model does not consider a latent period. We therefore assume that individuals recover and become susceptible again in an average of 28 days after infection (equivalently, with a recovery rate $\gamma = 1/28$ per day). This time interval corresponds approximately to the duration of the post-treatment prophylactic effect of a full course of chloroquine (CQ; total dose, 25 mg of base/kg over 3 days) and primaquine (PQ; 0.5 mg of base/kg/day for 7 days), the antimalarial drugs used for radical cure of vivax malaria in Brazil [1]. Remaining parameters were estimated by simultaneously fitting two sets of empirical data: (a) the age-specific malaria incidence density in the urban population of Mâncio Lima $(D_1 = \{(k, \tilde{y}_{1k})\}_{k=0}^{80})$ and (b) the number of vivax malaria episodes notified per urban resident over 12 months of follow-up $(D_2 = \{(k, \tilde{y}_{2k})\}_{k=0}^{6})$. This approach contrasts with previous attempts to fit similar SIS models to age-related malaria prevalence or incidence data in that we also consider the overall frequency distribution of malaria episodes in the population [2, 3]. First, assuming equilibrium conditions, the system of ODEs was simulated, in age domain, from age 0 to 80 in order to generate incidence profiles over age and risk group. Next, we reprofiled incidence over age according to the population age structure determined by our census survey and computed a distribution of the number of cases experienced per person over 12 months. Parameter estimation was performed with the software Matlab, using PESTO (Parameter EStimation Toolbox; [4]). We assume that the residuals between model outputs and data are normally distributed, with unknown standard deviations. Our optimisation process maximized the likelihood (Equation S1) of observing both datasets, that is,

$$L(D_1, D_2, \theta) = \prod_{k=0}^{80} \frac{1}{\sigma_1\sqrt{2\pi}} \exp\left(-\frac{\left(\tilde{y}_{1k} - y_1(k)\right)^2}{2\sigma_1^2}\right) \cdot \prod_{k=0}^{6} \frac{1}{\sigma_2\sqrt{2\pi}} \exp\left(-\frac{\left(\tilde{y}_{2k} - y_2(k)\right)^2}{2\sigma_2^2}\right), \quad \text{(S1)}$$

in which y_1 is the model output for age-specific malaria incidence densities, y_2 is the model output for the number of cases per person over 12 months, σ_1 is the standard deviation of the measurement noise for y_1, and σ_2 is the standard deviation of the measurement noise for y_2. We optimized the model fitting considering that the HR group comprised 10%, 15%, 20%, 25% or 30% of the hosts; although where exactly we partition what is conceivably a continuous risk distribution is somewhat arbitrary we informed this selection on likelihood values. To ensure that the observed maximum is global, we performed 30 multi-starts initialised with randomly sampled parameter values following a Latin hypercube. We also used PESTO to derive 95% credible intervals for each parameter by using Monte-Carlo Markov Chain methods considering 10^5 iterations.

References

1. Ministry of Health of Brazil. Practical guidelines for malaria therapy [in Portuguese]. Brasília, Ministry of Health of Brazil. Brasília, Brazil: Ministry of Health of Brazil; 2010. Available from: http://bvsms.saude.gov.br/bvs/publicacoes/guia_pratico_malaria.pdf.
2. Águas R, White LJ, Snow RW, Gomes MGM. Prospects for malaria eradication in sub-Saharan Africa. PLoS ONE 2008; 3: e1767.

3. White MT, Walker P, Karl S, Hetzel MW, Freeman T, Waltmann A, et al. Mathematical modeling of the impact of expanding levels of malaria control interventions on *Plasmodium vivax*. Nat Commun 2018;9:3300.
4. Stapor P, Weindl D, Ballnus B, Hug S, Loos C, Fiedler A, et al. PESTO: Parameter EStimation TOolbox. Bioinformatics 2018 15;34:705-707.